Microchimica Acta (2019) 186:843
https://doi.org/10.1007/s00604-019-3993-5

ORIGINAL PAPER

Switchable DNA tweezer and G-quadruplex nanostructures for ultrasensitive voltammetric determination of the K-ras gene fragment

Haohan Chen[1] · Xiaofan Sun[1] · Rongfeng Cai[1] · Yaping Tian[1] · Nandi Zhou[1]

Received: 11 July 2019 / Accepted: 30 October 2019

Abstract
Voltammetric detection of the K-ras gene fragment was accomplished through the combined application of (a) a switchable DNA nanostructure, (b) the use of hairpin probe and exonuclease III (Exo III)-assisted signal amplification, (c) a split G-quadruplex, and (d) by exploiting the redox activity of DNAzyme. Three assistant oligonucleotides were designed to construct a DNA tweezer on a gold electrode. It is in "open state" in the absence of K-ras DNA. Then, a hairpin probe was introduced, whose stem-loop structure can be opened through hybridization with the K-ras DNA. Exo III is added which hydrolyzes the complementary region of the hairpin sequence to release a single-stranded rest fragment. The ssDNA hybridizes with the DNA tweezer on the electrode which thereby is switched to the "closed state". This leads to the formation of G-quadruplex due to the shortened distance of the split G-quadruplex-forming sequences in the tweezer. The voltammetric signal of the G-quadruplex-hemin complex, with a peak near −0.3 V vs. Ag/AgCl, is used as the signal output. Under the optimal conditions, the current response in differential pulse voltammetry (DPV) increases linearly with the concentration of K-ras DNA in the range of 0.01–1000 pM, and the detection limit is 2.4 fM. The assay can clearly discriminate K-ras DNA from a single-base mutation. The method has excellent selectivity and was applied to the determination of K-ras DNA in (spiked) serum samples.

Keywords Electrochemical DNA biosensor · Target recycling amplification · Differential pulse voltammetry · Hemin · Gold electrode · Electrochemical impedence spectroscopy · Human serum samples

Introduction

The concentration of target DNA in biological samples is usually very low, and ultrahigh sensitivity is therefore essential for successful detection [1, 2]. For DNA biosensors based on hybridization between the complementary sequences, different signal amplification strategies are applied to improve sensitivity [3, 4]. These signal amplification strategies can generally be classified into two types. One is the use of nanomaterials as direct signal probes or the carriers of signal labels [5–7]. Among various nanomaterials available, gold nanoparticles, graphene and the derivatives, carbon nanotubes and metal oxide nanomaterials have significant contribution in the development of biological sensing technology owing to their unique excellent features. The other is biological amplification technologies, including polymerase chain reaction amplification [8], chain displacement amplification [9], rolling ring amplification technique [10], hybrid chain reaction amplification [11, 12], nuclease-assisted amplification [13, 14], etc., which are generally based on the polymerization, hybridization, nicking or hydrolysis of nucleic acids. Although these strategies have significantly enhanced the detection sensitivity, robust assays with high sensitivity, high specificity and low-cost for sequence-specific DNA are still greatly desired [15].

Self-assembly technology acts an important role in modern nanotechnology, which aims to develop nanoscale components, equipments and systems with low cost. Self-assembly can be used to aggregate individual atoms, molecules, or super-molecular blocks and form useful structures [16].

✉ Nandi Zhou
zhounandi@jiangnan.edu.cn

[1] The Key Laboratory of Carbohydrate Chemistry and Biotechnology, Ministry of Education, School of Biotechnology, Jiangnan University, Wuxi 214122, China

Published online: 25 November 2019

DNA nanotechnology relies on the interaction of specific sequences, combining the complementary oligonucleotides into a double helix. Diverse DNA nanostructures can thus be constructed through self-assembly of a set of well-designed oligonucleotides, and sometimes can be activated by specific signal molecules or environment factors [17, 18]. DNA nanostructures with specific functions are named as DNA molecular machines, such as autonomous walking machine [19], nano-tweezers [20, 21] and nano-cages [22], etc. Owing to the molecular recognition characteristics of DNA (acts as complementary sequence or aptamer), these DNA molecular machines have been used to construct biosensing systems and shown promising applications [23–26]. Among the reported DNA nanostructures, DNA tweezer has controllable structure which can be switched between open state and close state depending on the existence of the targets, and therefore has been widely used in biosensing configuration [27–29]. For example, a switchable DNA nanotweezer biosensor was fabricated for the detection of PML/RARα, which achieved high sensitivity [30]. And a double-crossover motif-based DNA nanotweezer was designed for logic gate building and biosensing of microRNAs [31].

K-ras proto oncogene is one of the members of ras family that regulates cell growth as a molecular switch. The codon 12 mutation will disorder cell growth and cause cancer. According to statistics, approximately 70–90% of pancreatic cancer cases indicated K-ras mutations [32]. Therefore, the detection of K-ras is of great significance since it can be utilized as a biomarker in the early diagnosis of pancreatic cancer [33, 34]. Herein, taking K-ras gene as an example, we construct an ultrasensitive electrochemical biosensor for sequence-specific DNA through the combination of exonuclease III-assisted signal amplification and the configuration of switchable DNA tweezer and G-quadruplex structure on the electrode. The nano-tweezer switches to close state from open state when specific DNA is present, forming G-quadruplex on the electrode. The rationally designed biosensor exhibits both high sensitivity and high specificity.

Experimental

Materials and reagents

Human serum was purchased from Beijing Solarbio Science & Technology Co., Ltd. 6-mercaptohexanol (6-MCH) and hemin were purchased from Sigma-Aldrich. Exonuclease III (Exo III) was purchased from Takara Biotechnology Co., Ltd. 4-(2-hydroxyethyl)-1-piperazine ethanesulfonic acid sodium salt (HEPES) was obtained from Sangon Biotech Co., Ltd. All other reagents used were in analytical grade, and the solutions were prepared with ultrapure water (18.2 MΩ cm) from a Millipore water purification system.

The HPLC-purified customized oligonucleotides were provided by Sangon Biotech Co., Ltd., which were dissolved in 10 mM phosphate buffered saline (containing 1 M NaCl, 1 mM $MgCl_2$, pH 7.4) before use. The sequences of the oligonucleotides were as below.

A1: 5′-HS-CCGACCGCAGGATCCTATAACTTGACGTAGCTAGAAGGAG-3′

A2: 5′-GCTGGTGGCGTAGGCAAGATACATTTTACGCCTGGTGCC-SH-3′

A3: 5′-GGGTTGGGTTTTTATAGGATCCTGCGGTCGGAGGCACCAGGCGTAAA ATGTATTTGGGTAGGG-3′

Hairpin probe: 5′-TCACTCCTTCTAGCTACGTCAAGGCACTCTTGCCTACGCCA CCAGCTCCAACTTGTGGTAGTTGGAGCTGGTGGCGTAGGCAAGAGTGCCTTGACGA-3′

K-ras DNA: 5′-TCGTCAAGGCACTCTTGCCTACGCCACCAGCTCCAACTACCA CAAG-3′

Single-base mismatched K-ras DNA: 5′-TCGTCAAGGCACTCTTGCCTACGCCA CCAGCTCCAACTACC**C**CAAG-3′

Three-base mismatched K-ras DNA: 5′-TCGTCAAGGCACTCTTGCCTACGCCAC CAGCTCCAACTAC**A**C**A**AAG-3′

The underlined, bold underlined, double underlined, wavy underlined and break underlined letters are the respective complementary sequences, and the bold letters are the mismatched bases.

Preparation of the tweezer-modified gold electrode

Gold electrode (3 mm) was polished with 0.5 and 0.05 μm Al_2O_3 powder and sonicated in absolute ethanol and water. And then, the electrode was subjected to electrochemical pretreatment by consecutive potential cycling in 0.5 M H_2SO_4 solution within a potential window between −0.2 V and +1.5 V. After that, the electrode was rinsed with water and dried at nitrogen atmosphere.

To form DNA tweezer structure, the same concentration (0.8 μM) of the sequences A1, A2 and A3 were mixed and incubated at 95 °C for 5 min, and cooled down to room temperature in 2 h. After the self-assembly of DNA tweezer structure, gold electrode was immersed in 100 μL of the above solution for 6 h, allowing the attachment of the tweezer on the surface of gold electrode via the two thiol groups of the tweezer. Then the tweezer-modified electrode was thoroughly washed with 10 mM phosphate buffer and dried with nitrogen. The electrode was finally blocked with 2 mM 6-MCH for 4 h, rinsed with 10 mM phosphate buffer and gently dried with nitrogen.

A CHI 660e electrochemical workstation was used to perform all electrochemical measurements with a typical three-electrode system. The modified gold electrode was employed

as working electrode, with a platinum wire counter electrode, and an Ag/AgCl reference electrode. Electrochemical impedence spectroscopy (EIS) were carried out in 0.1 mM $[Fe(CN)_6]^{3-/4-}$ (containing 0.1 M KCl) to characterize the different interfacial processes during the modification of the electrode in the frequency range from 0.1 Hz to 10 kHz.

Exo III-assisted amplification and hybridization with tweezer structure

Samples containing different concentrations of K-ras sequence were mixed with 0.6 μM hairpin probe dissolved in 100 μL hybridization solution, kept at 95 °C for 5 min, and cooled down to room temperature. Add 60 U of Exo III to the above hybridization solution and digest it for 2 h. And then, the tweezer-modified gold electrode was immersed in the above solution for 2 h to allow pairing of the complementary bases. After that, the electrode was thoroughly rinsed with 10 mM phosphate buffer to remove physically adsorbed substance.

Electrochemical determination based on formed G-quadruplex-hemin complex

The modified electrode was firstly treated with G-quadruplex forming solution (10 mM HEPES containing 50 mM KCl, pH 8.0) for 30 min to form G-quadruplex. Then 200 μM hemin was added and the electrode was further treated for 1 h to form the desired G-quadruplex-hemin complex.

Differential pulse voltammetry (DPV) was carried out in 20 mM HEPES buffer (containing 20 mM KCl, pH 8.0) within the potential range of −0.6~−0.15 V, with the increasement of 0.004 V, amplitude of 0.05 V, pulse width of 0.05 s. Prior to determination, the buffer was bubbled thoroughly with high purity nitrogen for 30 min. And a stream of nitrogen was blown gently across the surface of the test buffer throughout the determination. The peak current at −0.3 V from G-quadrupelx-hemin complex, was recorded and used to quantify the concentration of K-ras DNA.

Results and discussion

Designed strategy of the electrochemical biosensor

The DNA tweezer and Exo III-assisted electrochemical assay for sequence-specific DNA is depicted in Scheme 1. A special tweezer containing two split G-quadruplex-forming sequences and a hairpin probe (Hp) were customized to achieve the mechanism.

The tweezer structure is formed through the self-assembly of three oligonucleotides A1, A2 and A3. A1 consists of segment 1 and 2, and a thiol group at its 5′-end. A2 consists of segment 3 and 4, and a thiol group at its 3′-end. A3 consists of four regions: segment 5 and 6, and two split G-quadruplex-forming sequences at its 5′-end and 3′-end, respectively. Among these segments, segment 1 and 5 are complementary sequences, whereas segment 4 and 6 are complementary sequences. Therefore, after equimolar incubation and self-assembly, a tweezer structure in its open state can be formed, with a pair of thiol groups at its terminal. The two split G-quadruplex-forming sequences in open state tweezer are far away from each other, and thus cannot form a complete G-quadruplex structure. The tweezer is then modified on gold electrode through its thiol group pair.

Then a hairpin probe consists of segment 7, 8 and 9 is designed, where segment 7 is complementary to segment 2, segment 8 is complementary to segment 3, and segment 9 is complementary to the target, K-ras gene sequence. Moreover, segment 8 and 3′-end of segment 7 are designed to be complementary to 3′-end of segment 9, which allows the stability of the stem-loop structure of the hairpin probe in the absence of K-ras sequence. When the target DNA was presence, it hybridized with the hairpin probe, opened the stem-loop structure, and formed a duplex DNA. Then Exo III catalyzed the cleavage of Hp/K-ras duplex, which released a short ssDNA consists of segment 7 and 8, together with K-ras sequence for the next round of hybridization with Hp. The hybridization, cleavage and releasing cycle achieves intensive signal amplification by producing a large amount of short ssDNA.

Finally, the produced short ssDNA is allowed to hybridize with the tweezer structure modified on the electrode through the complementary sequences between segment 2 and 7, and segment 3 and 8. The hybridization switches the tweezer to a close state, where the two split G-quadruplex-forming sequences become closer. After incubation in G-quadruplex forming solution and further introduction of hemin, G-quadruplex-hemin complex can be formed due to the insertion of hemin into G-quadruplex. And then, DPV was carried out under the conditions previously described. Developed on the basis of classical voltammetric analysis, DPV has reduced background current and high sensitivity, thus has been widely employed in quantitative electrochemical analysis. The electrochemical response is related to the amount of G-quadruplex-hemin complex, that is, positively correlated with the concentration of target DNA.

Verification of the feasibility of the principle

In order to verify the feasibility of the experimental principle, gel electrophoresis, electrochemical impedance spectroscopy (EIS) and DPV experiments were carried out.

The polyacrylamide gel electrophoresis image in Fig. 1 verifies the formation of DNA tweezer nanostructure and the achievement of Exo III-assisted amplification. Compared with the bands in lane 1, 2 and 3, which represent DNA probe A1,

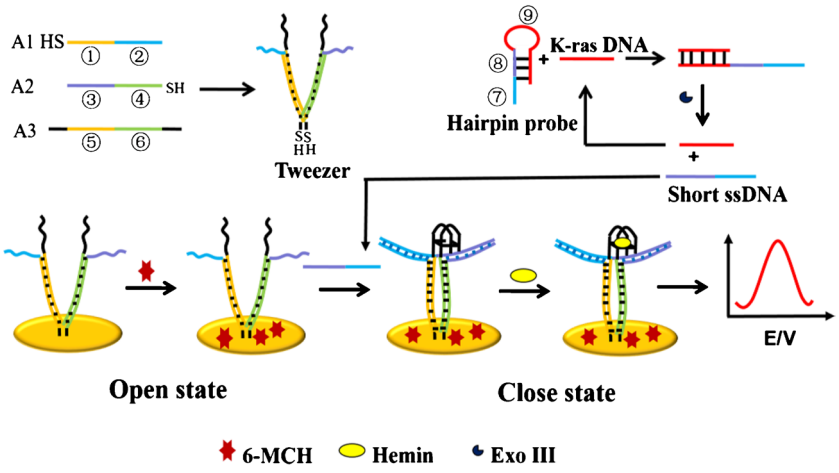

Scheme 1 Principle of the electrochemical determination of target DNA based on tweezer structure and Exo III-assisted amplification. K-ras DNA is hybridized with hairpin probe and then digested by exonuclease III (ExoIII), producing short ssDNA. The later can combine with the DNA tweezer through hybridization and switch the tweezer from open state to close state. The subsequently formed G-quadruplex-hemin complex is used as the output signal

A2 and A3 respectively, the band in lane 4 with higher molecular weight indicates the formation of the DNA tweezer. Whereas the bands in lane 5 and 6 represent the hairpin probe and K-ras DNA, the bands in lane 7 indicate the duplex of the hairpin probe/K-ras DNA and the produced short ssDNA. Therefore, the Exo III-assisted amplification is confirmed.

Electrochemical impedance spectroscopy (EIS) is a frequently used method to characterize the modification of the electrodes. Figure 2a shows the EIS curves of different modified gold electrode. Because of the electrostatic repulsion of the tweezer DNA against $[Fe(CN)_6]^{4-/3-}$, the electron transfer resistance (R_{et}) in curve b is apparently larger than that of bare gold electrode (curve a). R_{et} of the electrode is greatly enhanced (curve c) after it is blocked with 6-MCH. The above results confirms that the modification of the electrode is successful.

With the switching of the tweezer structure from open state to close state, the G-quadruplex-hemin complex formed. It

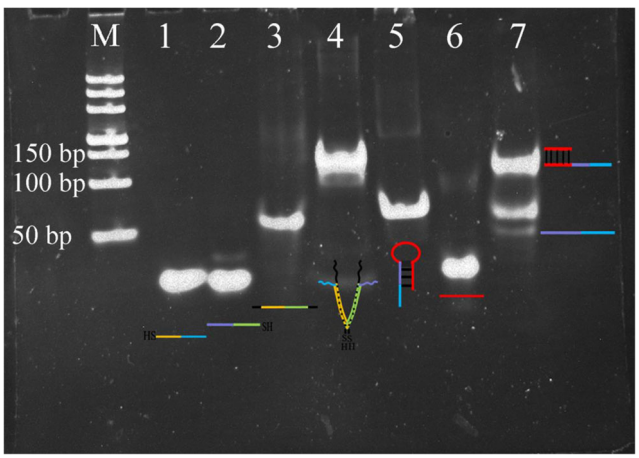

Fig. 1 Polyacrylamide gel electrophoresis image (Run polyacrylamide gel for 40 min at a voltage of 120 V). Lane M: DL500 DNA ladder; Lane 1: DNA probe A1; Lane 2: DNA probe A2; Lane 3: DNA probe A3; Lane 4: after incubation of DNA probe A1/A2/A3; Lane 5: hairpin probe; Lane 6: K-ras DNA; Lane 7: products after incubation of hairpin probe, K-ras DNA and Exo III

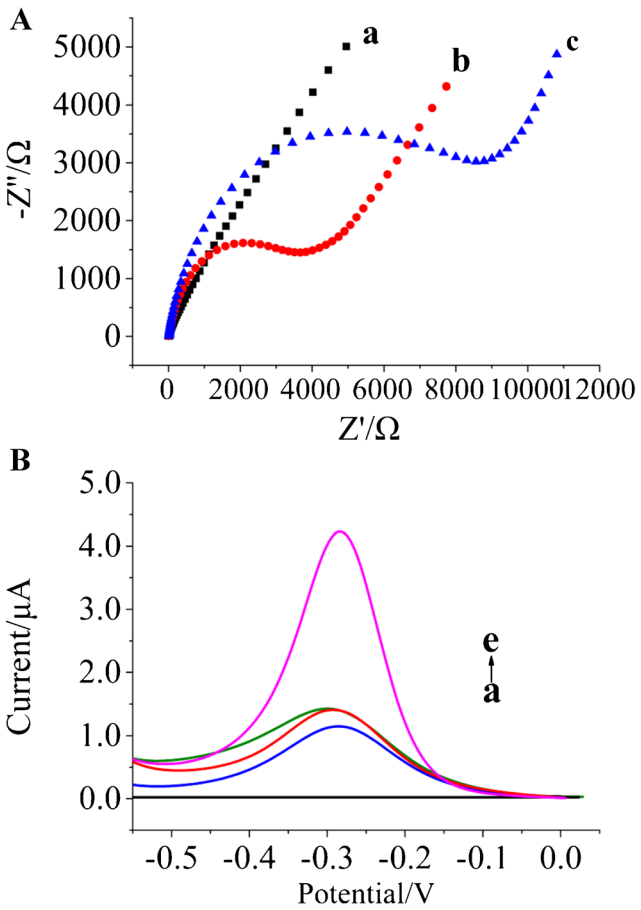

Fig. 2 (*A*) Characterization of the modification of the electrode by EIS within the frequency range of 0.1 Hz to 100 K Hz at amplitude of 5 mV: bare gold electrode (**a**); tweezer-modified gold electrode (**b**) and 6-MCH-blocked tweezer-modified gold electrode (**c**). (*B*) DPV curves in the presence of tweezer structure, hairpin probe, Exo III and K-ras DNA (**a**); hairpin probe, Exo III, K-ras DNA and hemin (**b**); tweezer structure, Exo III, K-ras DNA and hemin (**c**); tweezer structure, hairpin probe, K-ras DNA and hemin (**d**); tweezer structure, hairpin probe, Exo III, K-ras DNA and hemin (**e**). DPV was carried out in 20 mM HEPES buffer (containing 20 mM KCl, pH 8.0) within the potential range of −0.6~−0.15 V, with the increasement of 0.004 V, amplitude of 0.05 V, and pulse width of 0.05 s

was then utilized as signal molecular, owing to its electroactivity. To test the feasibility of the constructed biosensor, the electrochemical responses of the different combinations of components (0.8 μM tweezer structure, 0.5 μM K-ras DNA, 0.6 μM hairpin probe, 60 U Exo III and 200 μM hemin) were recorded and showed in Fig. 2. Apparently, the formation of G-quadruplex-hemin complex requires the coexistence of K-ras DNA, Hp, Exo III and hemin. Indeed, an obvious peak occurs in DPV curve in the presence of all these components (curve e), indicating the successful switching of the structure of the tweezer and the formation of G-quadruplex-hemin complex on the electrode surface. In those control experiments, the absence of the tweezer structure (curve b), Hp (curve c) or Exo III (curve d) causes much lowered peak current in DPV curves. Actually, the close state tweezer and subsequent G-quadruplex-hemin complex cannot be formed in the absence of any components. The background noise is due to the electrochemical response of hemin on the electrode, but the peak current is much lower than the current signal of the G-quadruplex-hemin complex. This can be proven by another control experiment. The DPV curve in the absence of hemin, yet in the presence of the tweezer, Hp, Exo III and K-ras DNA was also recorded (curve a), which shows that the electrochemical signal only can generate in the presence of hemin. Based on the these results, the principle of the electrochemical assay is feasible.

Optimization of the assay conditions

In order to achieve the highest sensitivity of the electrochemical biosensor, the experimental parameters such as the concentration of the tweezer-forming oligonucleotides, the hairpin probe and Exo III, and the incubation time of the produced short ssDNA with the tweezer were optimized.

The concentration of the nano-tweezer affects the number of the nano-tweezer, thereby the G-quadruplex-hemin complexes on the electrode, which ultimately affects the peak current of the DPV. Since the tweezer structure is consisted of A1, A2 and A3 probes through hybridization at a molar ratio of 1:1:1, the same concentration of the three oligonucleotides was utilized to construct the tweezer. Different concentrations of three oligonucleotides, ranging from 0.2 μM to 1.0 μM, were used to form tweezers to modify gold electrode. And the hybridization solution consists of 0.5 μM K-ras DNA, 0.5 μM Hp and 60 U Exo III. The tweezer-modified electrodes were then incubated with the hybridization solution and then with 200 μM hemin. Finally, the DPV curves were recorded and the relationship between the peak current in DPV and the concentration of the oligonucleotides was investigated. Figure 3a shows that the peak current increases with the increased concentration of oligonucleotides. When the concentration reaches 0.8 μM, the current value no longer increases. So, 0.8 μM is the appropriate concentration of A1, A2 and A3 probes.

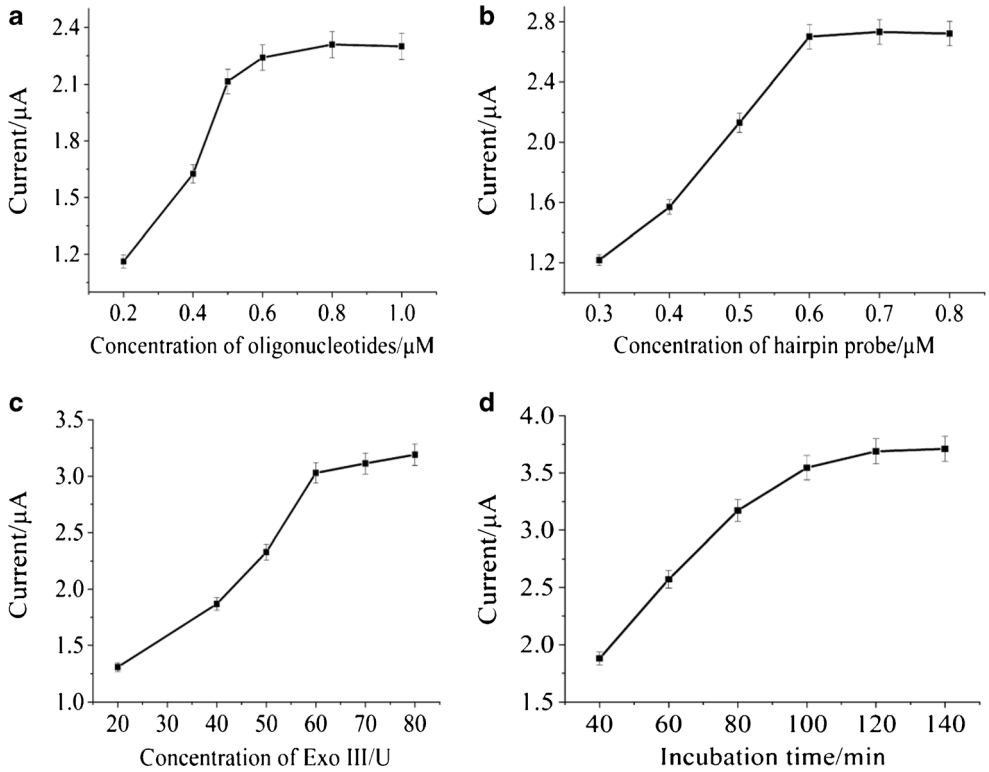

Fig. 3 Optimization of the assay conditions. DPV was carried out according to the conditions in Fig. 2B. The influence of (**a**) the concentration of tweezer-forming oligonucleotides, (**b**) the concentration of hairpin probe, (**c**) the concentration of Exo III, and (**d**) the incubation time on the peak current in DPV

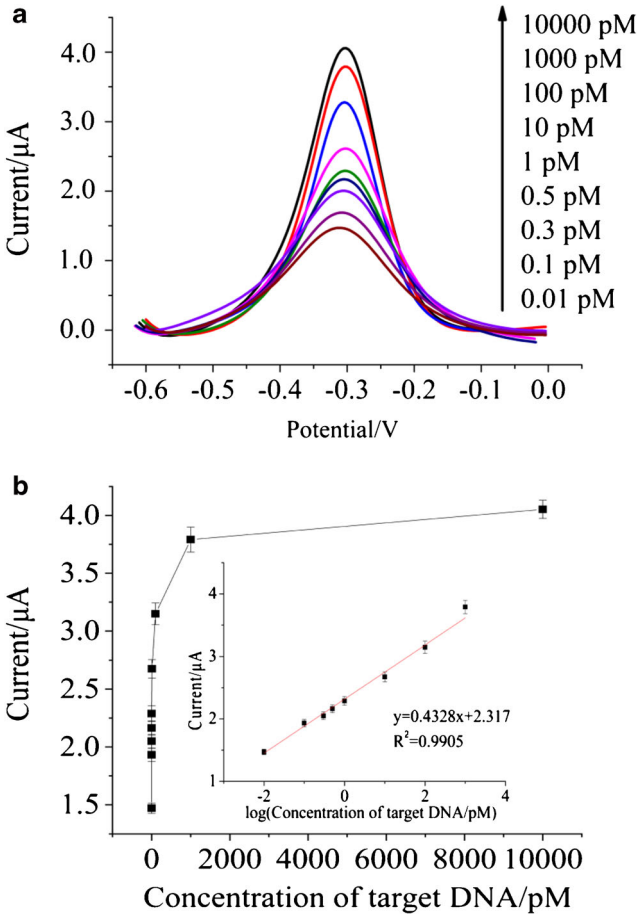

Fig. 4 (**a**) The DPV current gradually increases with the increasing concentration of K-ras DNA (ranging from 0.01 pM to 10,000 pM); (**b**) The relationship between the peak current in DPV and the concentration of target DNA; The inset shows the calibration plot of the current response vs. logarithm K-ras DNA concentration in the range from 0.01 pM to 10,000 pM. DPV was carried out according to the conditions in Fig. 2b

Then the influence of the concentration of hairpin probe was studied. The concentration of the hairpin probe influences the amount of the produced short ssDNA and therefore the amplification efficiency. Oligonucleotides of different concentrations of Hp, ranging from 0.3 μM to 0.8 μM, were employed in the solutions, and then DPV was conducted. Figure 3b shows that the peak current increases with the increased concentration of Hp. When the concentration reaches 0.6 μM, the current value no longer increases. So, the concentration of hairpin probe is fixed at 0.6 μM.

The concentration of Exo III influences the amount of the produced short ssDNA and the reaction time. The effect of Exo III concentration was studied by adding 20 U to 80 U of Exo III to the hairpin-target hybridization solution. Figure 3c shows that when Exo III is below 60 U, the current peak obviously increases with the increased amount of the enzyme. When the added Exo III exceeds 60 U, the increase rate of current peak reduces. Thus 60 U is the optimal concentration of Exo III.

Finally, the effect of the incubation time of the produced short ssDNA with the tweezer structure was investigated. The tweezer-modified electrode was immerse into the above Hp/K-ras/Exo III reaction solution. Different incubation times ranging from 40 min to 140 min were used to allow the hybridization between the produced ssDNA with the tweezer structure. Figure 3d shows that when the incubation time is extended, the peak current also gradually increases. When the incubation time reaches 120 min, the peak current increase tends to be flat, which means that the hybridization solution has reached saturation. Therefore, the incubation time of 120 min was chosen for the following experiments.

Performance of the electrochemical assay

To determine the dynamic response range of the electrochemical biosensor, different concentrations of K-ras DNA were used and detected under the optimal conditions. K-ras DNA was mixed into the solution containing 0.6 μM Hp, and additional 60 U Exo III. The mixture was then applied to the surface of the tweezer-modified gold electrode. After the electrode was treated with G-quadruplex forming solution, DPV was performed in the presence of hemin. In the range from 0.01 pM to 10,000 pM, the peak current of DPV curves enhances with the increase of concentration of K-ras DNA (Fig. 4a). The response range crosses over six orders of magnitude. Figure 4b reveals the relationship between the concentration of K-ras DNA and the peak current in DPV. From the calibration curve depicted in the inset of Fig. 4b, k-ras DNA

Table 1 An overview on recently reported nanomaterial-based optical or electrochemical methods for determination of DNA/RNA

Method applied	Materials used	Limit of detection	Detection range	Reference
Electrochemical(DPV)	Methylene blue	2.4 aM	0.0001~1 pM	[5]
Electrochemical(DPV)	HRP and GOx	0.03 fM	1~100,000 pM	[20]
Chemiluminescence	G-quadruplex-hemin complex ABTS	30 fM	0.1~10,000 pM	[21]
Fluorescence imaging method	Fluorescein/quencher	5.29 pM	10~10,000 pM	[27]
Fluorescent	Fluorescein/quencher	0.6 pM	1 ~500,000 pM	[28]
Colorimetric detection	G-quadruplex-hemin complex and ABTS	10 pM	10 ~150,000 pM	[35]
Electrochemical(DPV)	G-quadruplex-hemin complex	2.4 fM	0.01 ~1000 pM	This work

can be ultra-sensitively analyzed within 0.01–10,000 pM. The detection limit is estimated to be 2.4 fM (S/*N* = 3). The linear regression equation can be expressed as y = 0.4328*log C + 2.317, where y and C represent the peak current and concentration of K-ras DNA. A large number of G-quadrupelx-hemin complexes introduced on the closed state tweezer and the EXO III-assisted signal amplification contributed to the ultrahigh sensitivity of the biosensor. In order to evaluate the performance of the present sensing system, the assay results were compared with the results from other reported references, which were summarized in Table 1.

The specificity of the electrochemical biosensor was investigated. Figure 5 shows that the great difference in the peak current exists in the presence of the target sequence and mismatched sequences. A single base mutation in the sequence leads to only 20.7% of the original peak current. When the three base mutation occurs, the peak current is lower. Therefore, the fabricated electrochemical DNA biosensor has excellent specificity to clearly discriminate the slight differences of the gene, such as the mutation of K-ras gene, indicating its prospect in early diagnosis and monitoring of pancreatic cancer.

Quantitation of K-ras DNA in serum samples

To assess the practicability and interferent-resistance of the tweezer structure-based DNA sensor, K-ras DNA spiked serum samples were employed. A certain amount of the purchased serum was taken and centrifuged at 10,000 rpm for 3 min. Then the supernatant was mixed with 10 mM phosphate buffer at a ratio of 1:4 to obtain 5 times diluted serum. After that, different concentrations of K-ras DNA were added to the diluted serum to prepare K-ras DNA spiked serum samples. And the determination was carried out just the same as that for standard samples.

Figure 6a reveals that the higher peak current is obtained at the higher concentration of K-ras DNA in serum. In Fig. 6b, a gradual increase of the peak current is clearly observed along with the increasing concentration of K-ras DNA. A linear relationship between the peak current and the logarithm of the concentration of the K-ras DNA can be established from of 0.01–10,000 pM. The linear regression equation can be expressed as y = 0.2270*log C + 1.730, where y and C represent the peak current and concentration of K-ras DNA. The detection limit is estimated to be 5.4 fM (S/*N* = 3). Compared with the detection range and detection limit in solution, the

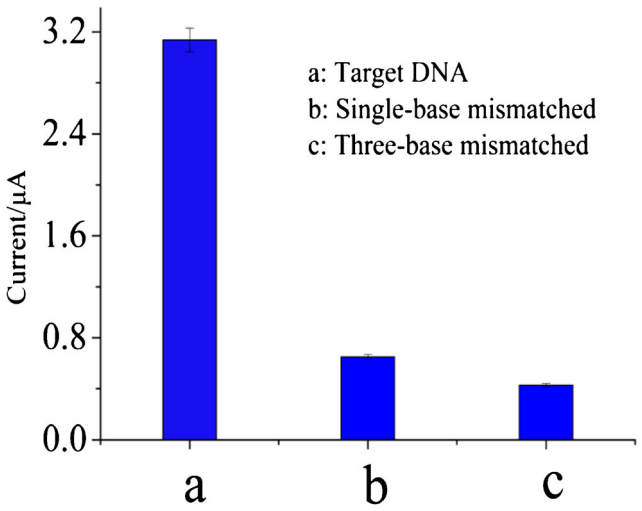

Fig. 5 Verification of the specificity of the method. The response of the electrochemical biosensor towards K-ras DNA, single-base mismatched K-ras DNA and three-base mismatched K-ras DNA. DPV was carried out according to the conditions in Fig. 2b

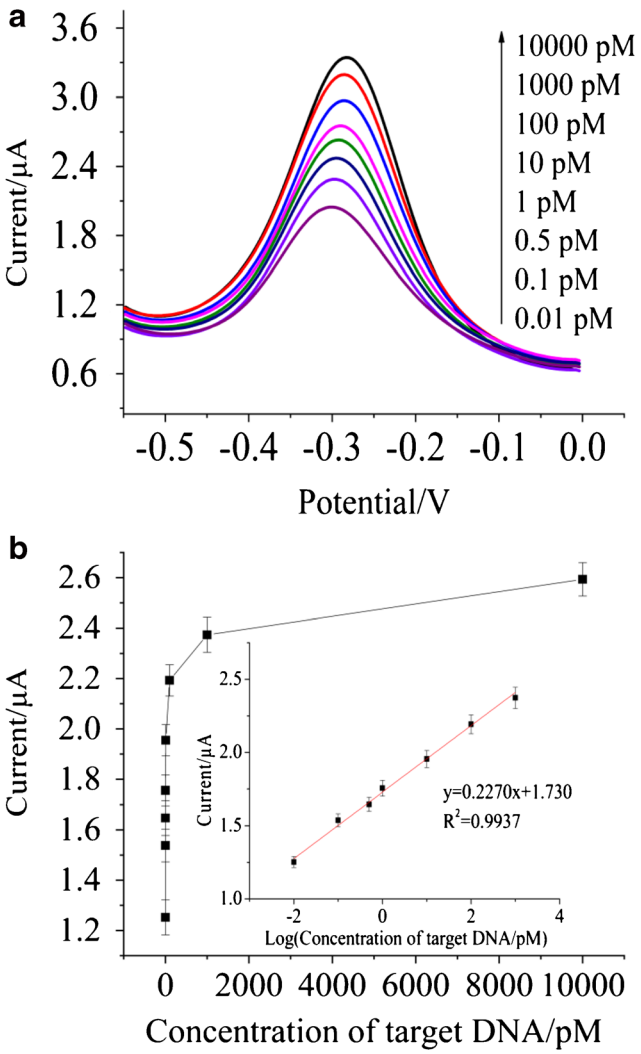

Fig. 6 (**a**) The DPV current gradually increases with the increasing concentration of K-ras DNA in serum samples (ranging from 0.01 pM to 10,000 pM); (**b**) The relationship between the peak current in DPV and the concentration of K-ras DNA in serum samples; The inset shows the calibration plot of the current response vs. the logarithm K-ras DNA concentration in serum samples in the range of 0.01 pM to 10,000 pM. DPV was carried out according to the conditions in Fig. 2b

data for serum samples show that serum has just a little disturbs the detection result. Therefore, it has excellent practicability in medical test. Overall, the method also has shortcomings, e.g. the construction of nano-tweezer is time-consuming; the introduction of the signal amplification target-recycling makes the detection system a bit complicated.

Conclusion

Through the combination of the concepts of switchable DNA nanostructure, hairpin probe and Exo III-assisted recycling signal amplification, split G-quadruplex sequence and redox activity of DNAzyme, an ultrasensitive electrochemical DNA biosensor was constructed to detect K-ras gene. The smart "off-on" design of DNA tweezer offers significant output signal, whereas Exo III-assisted recycling achieves high sensitivity. Although further effort may focus on the faster detection and simplified system, the fabricated DNA biosensor exhibits good practicability owing to its clear discrimination of single-base and three-base mismatched sequences from the target sequence and interferent-resistance in serum samples. Obviously, through the replacement of the tweezer and hairpin probe in this work to other customized sequences, the developed sensing strategy can easily be used to detect other biomarker genes and sequences. Therefore, the switchable DNA nanostructure-based electrochemical assay may have great application prospect in early diagnosis of gene-related diseases.

Acknowledgements This work was supported by the National Natural Science Foundation of China (no. 31271860), the Six Talent Peaks Project in Jiangsu Province (JY-078) and National First-class Discipline Program of Light Industry Technology and Engineering (LITE2018-07).

Compliance with ethical standards

Conflict of interest The author(s) declare that they have no competing interests.

Ethical approval All procedures were approved by medical ethics committee of Jiangnan University.

References

1. Zhang G, Tang Z, Wang W, Wu H, Maham A, Lin Y (2010) Hairpin DNA switch for ultrasensitive spectrophotometric detection of DNA hybridization based on gold nanoparticles and enzyme signal amplification. Anal Chem 82:6440–6446. https://doi.org/10.1021/ac1006238
2. Liu Z, Zhang W, Zhu S, Zhang L, Hu L, Parveen S, Xu G (2011) Ultrasensitive signal-on DNA biosensor based on nicking endonuclease assisted electrochemistry signal amplification. Biosens Bioelectron 29:215–218. https://doi.org/10.1016/j.bios.2011.07.076
3. Jing Z, Ding Y, Liu X, Wang L, Jiang W (2014) Toehold-mediated strand displacement reaction triggered isothermal DNA amplification for highly sensitive and selective fluorescent detection of single-base mutation. Biosens Bioelectron 59:276–281. https://doi.org/10.1016/j.bios.2014.03.051
4. Wei W, Ni Q, Pu Y, Yin L, Liu S (2014) Electrochemical biosensor for DNA damage detection based on exonuclease III digestions. J Electroanal Chem 714:25–29. https://doi.org/10.1016/j.jelechem.2013.12.018
5. Wang H, Ma R, Sun F, Jia L, Zhang W, Shang L, Xue Q, Jia W, Wang H (2018) A versatile label-free electrochemical biosensor for circulating tumor DNA based on dual enzyme assisted multiple amplification strategy. Biosens Bioelectron 122:224–230. https://doi.org/10.1016/j.bios.2018.09.028
6. Lei G, Sun X, Hong Q, Li F (2017) Ratiometric NanoCluster Beacon: a label-free and sensitive fluorescent DNA detection platform. ACS Appl Mater Interf 9:13102–13110. https://doi.org/10.1021/acsami.7b03198
7. Ge L, Wang W, Li F (2017) Electro-grafted electrode with graphene-oxide-like DNA affinity for ratiometric homogeneous electrochemical biosensing of microRNA. Anal Chem 89:11560–11567. https://doi.org/10.1021/acs.analchem.7b02896
8. Li Y, Miao X, Ling L (2015) Triplex DNA: a new platform for polymerase chain reaction – based biosensor. Sci Rep 5:13010. https://doi.org/10.1038/srep13010
9. Chen Q, Bian Z, Chen M, Hua X, Yao C, Xia H, Kuang H, Zhang X, Huang J, Cai G (2009) Real-time monitoring of the strand displacement amplification (SDA) of human cytomegalovirus by a new SDA-piezoelectric DNA sensor system. Biosens Bioelectron 24:3412–3418. https://doi.org/10.1016/j.bios.2009.06.012
10. Zhang Y, Wang L, Luo F, Qiu B, Guo L, Weng Z, Lin Z, Chen G (2017) An electrochemiluminescence biosensor for Kras mutations based on locked nucleic acid functionalized DNA walkers and hyperbranched rolling circle amplification. Chem Comm 53:2910–2913. https://doi.org/10.1039/c7cc00009j
11. Sun X, Chen H, Wang S, Zhang Y, Tian Y, Zhou N (2018) Electrochemical detection of sequence-specific DNA based on formation of G-quadruplex-hemin through continuous hybridization chain reaction. Anal Chim Acta 2012:121–128. https://doi.org/10.1016/j.aca.2018.02.076
12. Hou T, Li W, Liu X, Li F (2015) Label-free and enzyme-free homogeneous electrochemical biosensing strategy based on hybridization chain reaction: a facile, sensitive, and highly specific microRNA assay. Anal Chem 87:11368–11374. https://doi.org/10.1021/acs.analchem.5b02790
13. Li S, Chen A, Chai Y, Yuan R, Zhuo Y (2016) Electrochemiluminescence aptasensor based on cascading amplification of nicking endonuclease-assisted target recycling and rolling circle amplifications for mucin 1 detection. Electrochim Acta 212:767–774. https://doi.org/10.1016/j.electacta.2016.07.074
14. Zhou W, Gong X, Xiang X, Yuan R, Chai Y (2014) Quadratic recycling amplification for label-free and sensitive visual detection of HIV DNA. Biosens Bioelectron 55:220–224. https://doi.org/10.1016/j.bios.2013.12.021
15. Wu H, Zhang K, Liu Y, Wang H, Wu J, Zhu F, Zou P (2015) Binding-induced and label-free colorimetric method for protein detection based on autonomous assembly of gemin/G-quadruplex DNAzyme amplification strategy. Biosens Bioelectron 64:572–578. https://doi.org/10.1016/j.bios.2014.09.096
16. Li H, Carter JD, Labean TH (2010) Nanofabrication by DNA self-assembly. Mater Today 12:24–32. https://doi.org/10.1016/S1369-7021(09)70157-9
17. Jonathan B, Turberfield AJ (2007) DNA nanomachines. Nature Nanotech 2:275–284. https://doi.org/10.1038/nnano.2007.104

18. Liu M, Fu J, Hejesen C, Yang Y, Woodbury N, Gothelf K, Liu Y, Yan H (2013) A DNA tweezer-actuated enzyme nanoreactor. Nat Commun 4:2127. https://doi.org/10.1038/ncomms3127
19. Gu H, Chao J, Xiao S, Seeman N (2010) A proximity-based programmable DNA nanoscale assembly line. Nature 465:202–205. https://doi.org/10.1038/nature09026
20. Kou B, Chai Y, Yuan Y, Yuan R (2018) Dynamical regulation of enzyme cascade amplification by a regenerated DNA nanotweezer for ultrasensitive electrochemical DNA detection. Anal Chem 90: 10701–11076. https://doi.org/10.1021/acs.analchem.8b00477
21. Li D, Cheng W, Li Y, Li X, Yin X, Yin Y, Ju H, Ding S (2015) Catalytic hairpin assembly actuated DNA nanotweezer for logic gate building and sensitive enzyme-free biosensing of microRNAs. Anal Chem 88:7500–7506. https://doi.org/10.1021/acs.analchem.5b04844
22. Andersen E, Dong M, Nielsen M, Jahn K, Subramani R, Mamdouh W, Golas M, Sander B, Stark H, Oliveira C (2009) Self-assembly of a nanoscale DNA box with a controllable lid. Nature 459:73–76. https://doi.org/10.1038/nature07971
23. Zhang H, Lai M, Zuehlke A, Peng H, Li X, Le X (2016) Binding-induced DNA nanomachines triggered by proteins and nucleic acids. Angew Chem Int Ed 127:14534–14538. https://doi.org/10.1002/anie.201506312
24. Zhang P, Li Z, Wang H, Zhuo Y, Yuan R, Chai Y (2017) DNA nanomachine-based regenerated sensing platform: a novel electrochemiluminescence resonance energy transfer strategy for ultra-high sensitive detection of microRNA from cancer cells. Nanoscale 9:2310–2316. https://doi.org/10.1039/c6nr08631d
25. Liu S, Su W, Li Z, Ding X (2015) Electrochemical detection of lung cancer specific microRNAs using 3D DNA origami nanostructures. Biosens Bioelectron 71:57–61. https://doi.org/10.1016/j.bios.2015.04.006
26. Xu Z, Liao L, Chai Y, Wang R, Yuan R (2017) Ultrasensitive electrochemiluminescence biosensor for microRNA detection by 3D DNA walking machine based target conversion and distance-controllable signal quenching and enhancing. Anal Chem 89:8282–8287. https://doi.org/10.1021/acs.analchem.7b01409
27. Xu Y, Luo X, Geng N, Wu M, Lu Z (2018) DNA nanotweezers with hydrolytic activity for enzyme-free and sensitive detection of fusion gene via logic operation. J Anal Methods Chem 2018:7. https://doi.org/10.1155/2018/4178045
28. Gong X, Zhou W, Li D, Chai Y, Xiang Y, Yuan R (2015) RNA-regulated molecular tweezers for sensitive fluorescent detection of microRNA from cancer cells. Biosens Bioelectron 71:98–102. https://doi.org/10.1016/j.bios.2015.04.003
29. Funabashi H, Shigeto H, Nakatsuka K, Kuroda A (2015) A FRET-based DNA nano-tweezer technique for the imaging analysis of specific mRNA. Analyst 140:999. https://doi.org/10.1039/c4an02064b
30. Bian X, Guo B, Zhao M, Han D, Cheng W, Song F, Ding S (2019) An enzyme-free "ON-OFF" electrochemiluminescence biosensor for ultrasensitive detection of PML/RARα based on target-switched DNA nanotweezer. ACS AMI 11:3715–3721. https://doi.org/10.1021/acsami.8b18497
31. Li D, Wei C, Li Y, Xu Y, Li X, Yin Y, Ju H, Ding S (2016) Catalytic hairpin assembly actuated DNA nanotweezer for logic gate building and sensitive enzyme-free biosensing of microRNAs. Anal Chem 88:7500–7506. https://doi.org/10.1021/acs.analchem.5b04844
32. Yoshikawa K, Tanabe E, Shibata A, Inoue S, Kitayoshi M, Okimoto S, Fukushima N, Tsujiuchi T (2013) Involvement of oncogenic K-ras on cell migration stimulated by lysophosphatidic acid receptor-2 in pancreatic cancer cells. Exp Cell Res 319:105–112. https://doi.org/10.1016/j.yexcr.2012.09.014
33. Sun X, Wang S, Zhang Y, Tian Y, Zhou N (2017) Ultrasensitive detection of DNA based on target-triggered hairpin assembly and exonuclease-assisted recycling amplification. Sens Actuat B-Chem 252:306–312. https://doi.org/10.1016/j.snb.2017.06.014
34. Lin L, Liu A, Zhao C, Weng S, Lei Y, Liu Q, Lin X, Chen Y (2013) A chronocoulometric LNA sensor for amplified detection of K-ras mutation based on site-specific DNA cleavage of restriction endonuclease. Biosens Bioelectron 42:409–414. https://doi.org/10.1016/j.bios.2012.09.063
35. Xu H, Wu D, Li C, Lu Z, Liao X, Huang J, Wu Z (2017) Label-free colorimetric detection of cancer related gene based on two-step amplification of molecular machine. Biosens Bioelectron 90:314–320. https://doi.org/10.1016/j.bios.2016.12.003